Collisional Effects on Coherent Nonlinear Wave Particle Interactions for Second Harmonic Electron Cyclotron Heating

M.D. Carter, J.D. Callen, D.B. Batchelor and R.C. Goldfinger

March 1984

UWFDM-571

FUSION TECHNOLOGY INSTITUTE

UNIVERSITY OF WISCONSIN

MADISON WISCONSIN

Collisional Effects on Coherent Nonlinear Wave Particle Interactions for Second Harmonic Electron Cyclotron Heating

M.D. Carter, J.D. Callen, D.B. Batchelor and R.C. Goldfinger

Fusion Technology Institute
University of Wisconsin
1500 Engineering Drive
Madison, WI 53706

http://fti.neep.wisc.edu

March 1984

UWFDM-571

COLLISIONAL EFFECTS ON COHERENT NONLINEAR WAVE PARTICLE INTERACTIONS FOR SECOND HARMONIC ELECTRON CYCLOTRON HEATING

M.D. Carter, J.D. Callen, D.B. Batchelor* and R.C. Goldfinger*

Fusion Engineering Program
Nuclear Engineering Department
University of Wisconsin-Madison
Madison, Wisconsin 53706

March 1984

UWFDM-571

*Oak Ridge National Laboratory, Oak Ridge, TN 37830.

COLLISIONAL EFFECTS ON COHERENT NONLINEAR WAVE PARTICLE INTERACTIONS FOR SECOND HARMONIC ELECTRON CYCLOTRON HEATING

M.D. Carter and J.D. Callen

Fusion Engineering Program, Nuclear Engineering Department
University of Wisconsin, Madison, Wisconsin 53706

D.B. Batchelor and R.C. Goldfinger

Oak Ridge National Laboratory, Oak Ridge, Tennessee 37830

When electron orbits are trapped very near the second harmonic cyclotron resonance, quasilinear theory breaks down and nonlinear effects become important for particles with small $v_{\parallel}/v$. Numerical studies as well as a multiple time scale analysis demonstrate that relativistic detuning of the resonance for electrons is important even at low initial energies (~ 20 eV) resulting in periodic motion with large energy excursions on a time scale much longer than the gyrofrequency time scale. Small angle Coulomb collisions, parallel motion, and other processes randomize the nonlinear relativistic effects resulting in net heating. A Monte Carlo numerical model has been utilized to determine the net electron heating that results and to indicate the possible effects on electron energy distribution functions. Analytic formulae are derived describing the energy excursion behavior and heating in a mildly relativistic limit.

The usual quasilinear theory of cyclotron resonance heating assumes the wave-particle interaction to be sufficiently weak that on the time scale of interest the particle orbit does not deviate significantly from the unperturbed orbit. Also, it is assumed that the heating is stochastic due to the particle's passing repeatedly through a thin resonance zone, with the gyrophase relative to the wave randomized between successive passages. The energy evolution of such a stochastic orbit is shown in Fig. 1a. When the resonance occurs near the bottom of a magnetic well, deeply trapped particles essentially never leave the resonance zone so that the gyrophase is not randomized and energy excursions can occur which are large compared to the particle's initial energy. In this case, quasilinear theory breaks down, nonlinear orbit effects become important and for electrons, detuning due to the relativistic mass shift is crucial even at very low energies. Earlier numerical work by Batchelor and Goldfinger[1] demonstrated a transition as $v_{\parallel}/v$ at the midplane is reduced, from stochastic heating with small, random quasilinear energy steps to a coherent, periodic motion with large energy excursions for $v_{\parallel}/v = 0$. Such nonlinear effects on particle orbits may be important in the case of hot electron ring formation in EBT (Elmo Bumpy Torus),[2] or in tandem mirror schemes using second harmonic electron cyclotron heating to modify thermal barrier electron distribution functions.

An earlier nonrelativistic analysis[3] found exponential growth in energy for particles in a uniform magnetic field subjected to a perpendicularly propagating wave with a frequency of twice the gyrofrequency. Numerical solutions of the relativistically correct Lorentz equations for electrons in a uniform magnetic field show, however, that the exponential behavior is sustained for only a few growth periods. As the energy increases, the relativis-

tic phase slippage becomes important, detuning the resonance so that the energy saturates and eventually returns to near its initial value. This process is repetitious, resulting in large energy excursions but no continuous energy gain, as seen in Fig. 1c. For an electron which is deeply trapped in a magnetic well near the second harmonic resonance, transitions may also occur between the quasilinear behavior and the energy excursion behavior, as seen in Fig. 1b. The step size during the stochastic behavior of transitional electrons may also be comparable to their energy. The regions of phase space where energy excursions and transitions occur is shown qualitatively in Fig. 2, for a parabolic magnetic well.

The periodic behavior of electrons with no parallel energy does not constitute heating; however, randomizing events such as Coulomb collisions and a small amount of parallel motion can provide entropy production mechanisms. It is the purpose of this work to evaluate the actual nonlinear heating for electrons which violate the assumptions of quasilinear theory by utilizing a Monte Carlo code which includes Coulomb collisional effects. Also, the relativistic effects giving rise to the periodic energy excursions will be illustrated through a simple analytic model.

The Monte Carlo code used to study the effect of this phenomenon on a distribution of electrons integrates the Lorentz equations of motion:

$$\frac{d}{dt}(\gamma \underset{\sim}{v}) = -\frac{e}{mc}(\underset{\sim}{v} \times \underset{\sim}{B}) - \frac{e\underset{\sim}{E}}{m}, \tag{1a}$$

$$\frac{d}{dt}(\gamma) = -\frac{e\underset{\sim}{E}\cdot\underset{\sim}{v}}{mc^2}, \tag{1b}$$

where c is the speed of light, m the rest mass of the electron, e the magnitude of electron charge (positive), $\underset{\sim}{v}$ the electron velocity vector, $\underset{\sim}{E}$ is the rf electric field, $\gamma = [1 - v^2/c^2]^{-1/2}$, and v the magnitude of the velocity. The rf fields are determined by Maxwell's equations for an extraordinary mode in one of two magnetic field geometries. The first is a divergence-free, curl-free parabolic well: $\underset{\sim}{B} = B_0[(1 + (z^2 - x^2)/(L^2)]\,\hat{z} - (2xz)/(L^2)\,\hat{x}$. The second type of geometry is a divergence-free sinusoidal bumpy cylinder: $\underset{\sim}{B} = B_0\{[(1 + R)/2] + [(1 - R)/2]\cos(\pi z/L)\}\hat{z} + [(B_0\pi)/2L][(1 - R)/2]\sin(\pi z/L)\{x\hat{x} + y\hat{y}\}$ where B_0 is the midplane magnetic field strength, R is the mirror ratio and L is the axial magnetic field scale length, with the particles started on a field line near $x,y \sim L$. Integration of Eq. (1) is performed by using an Adams predictor-corrector routine on a gyrofrequency time scale. The accuracy of the integration is required to be less than a small fraction ($\sim 0.1\%$) of the smallest Coulomb collisional process. A 64 particle ensemble is followed, utilizing vectorization when possible to gain a roughly 15 fold increase over the sequential speed.

Small angle Coulomb collisions are modeled by scattering the test particles with a Maxwellian background plasma in three basic steps.[4,5] First, a rotation is made to a velocity space coordinate system with the axis along the velocity vector. In this new frame the solution to the Fokker-Planck equation in a uniform plasma for a delta function distribution of test particles is applied in a Monte Carlo sense. The following equation is used:

$$\underset{\sim}{v} = v_0\hat{z}[1 - \nu_s\delta t + \eta_1(\nu_{\parallel}\delta t)^{1/2}] + \eta_2 v_0(\nu_{\perp}\delta t)^{1/2}[\hat{x}\cos(2\pi\eta_0) + \hat{y}\sin(2\pi\eta_0)]\,,$$

where δt is the time since the last collision. In this equation only, the

perpendicular and parallel subscripts refer to the direction with respect to the initial velocity vector, not $\underline{B}$, and the collision frequencies, $\nu_\perp$ and $\nu_\parallel$, may be found in Ref. 4. The random number, η_0, is between 0 and 1, while η_1 and η_2 are random numbers from a normal (Gaussian) distribution chosen by Box-Muller sampling methods.[6] The transformation utilized in step 1 is then inverted to return the new scattered velocity to the coordinate system used to describe the magnetic fields.

The phase of the particle with respect to the wave determines whether the electron begins at the maximum of the energy excursion, the minimum, or somewhere in between. Hence, the energy evolution is phase dependent. Also, during the low energy part of an energy excursion, Coulomb collisions are more important so that the scattering of electrons into and out of the excursion region of velocity space is complicated. Thus, collisional effects are twofold with one effect providing a randomizing process for the test particle phase and the other determining the number of particles which are pitch angle scattered into the region of velocity space where nonlinear effects are important.

Figure 3 shows the dependence of the second harmonic heating coefficient on the ratio of an effective collision frequency to the energy excursion frequency. The dimensionless heating coefficient, α, is defined in terms of the average power absorbed per electron by those electrons with $v_\parallel/v$ at the midplane of less than 0.2. The defining equation is:

$$\text{ABSORBED POWER} \equiv \left\langle \frac{\partial T}{\partial t} \right\rangle \equiv \alpha \frac{e^2 \langle (k\rho)^2 \rangle |E_+|^2}{8\pi m \omega} \tag{2}$$

where k is the perpendicular wave number, ω is the radian wave frequency,

$\rho = v_\perp/\Omega_o$ is the electron gyroradius and $|E_+|$ is the magnitude of the right hand circularly polarized component of the wave. The <> brackets indicate that the enclosed quantity is calculated based upon the time averaged (~ 1 microsecond) parameters of only those electrons with $v_\parallel/v$ at the midplane less than 0.2. A wide range of collisionality was explored numerically for particle energies less than 2.5 keV and the analytical estimate which is derived later is shown by the dashed curve. Figure 3 demonstrates that Coulomb collisions can provide a significant enhancement of the effective heating due to the second harmonic resonance so long as the collisions do not completely annihilate the energy excursion behavior. Some phase randomizing process is necessary, however, for significant heating due to the nonlinear relativistic processes. This is not to say that the distribution function will not be affected by the presence of the wave in a collisionless regime, but that as many electrons will then lose energy as will gain energy.

Figure 4 demonstrates the ability of the second harmonic interactions to feed electrons from the cold background plasma to intermediate energies (~ 1 keV) by showing the energy distribution of 64 electrons averaged over a 1.1 microsecond time interval after approximately 9 microseconds. All the electrons were started at 205 eV. Background plasma parameters were chosen to resemble the T-mode of operation in EBT. A significant number of these electrons have been heated to form a tail on the distribution which can be compared with the Maxwellian background distribution shown as a dashed curve in Fig. 4. These tail electrons have very small pitch angle and most of the change in the distribution is due to the presence of the second harmonic resonance at the midplane. For this case the feed rate from 200 eV to ~ 1 keV is estimated to be about 1-5 x 10^{14} electrons per cm^3 per sec. The ratio of

collision to excursion frequencies corresponds to a value of about 1 in Fig. 3. Figure 3, however, accounts only for Coulomb collisional effects and it should be noted that any phase randomizing process could replace the collisional process. For the parameters in Fig. 4 the total second harmonic power absorbed by the electrons in an EBT-sized mirror cell is a few kilowatts.

The importance of relativistic detuning and an illustration of the relevant time scales involved can be obtained by a multiple time scale analysis resulting in a set of reduced "guiding center like" equations[7] for the energy excursion behavior, and which can be solved in a mildly relativistic limit. This developement parallels the non-relativistic treatment by Hsu and Chiu.[3]

Consider an electron in a uniform magnetic field, $\underset{\sim}{B} = B_0\hat{z}$, subjected to an electrostatic plane wave, $\underset{\sim}{E} = E_0\hat{x}\sin(kx - \omega t)$. Note that this wave is propagating perpendicular to $\underset{\sim}{B}$ with wave number k and frequency ω, which will be taken to be twice the gyrofrequency of the particle, to within a relativistic tuning factor. By considering this simple electromagnetic field description and defining new variables $u_\perp$ and Ψ such that $u_x \equiv (\gamma v_x/c) \equiv u_\perp \cos\Psi$, $u_y \equiv (\gamma v_y/c) \equiv u_\perp \sin\Psi$, and considering $u_z = 0$ for convenience, the equations of motion [Eq. (1)] can be written as:

$$\frac{du_\perp}{d\theta} = -\varepsilon \sin(\eta X - \theta)\cos\Psi$$

$$u_\perp \frac{d\Psi}{d\theta} = \frac{\Omega_0}{\gamma\omega} u_\perp + \varepsilon \sin(\eta X - \theta)\sin\Psi$$

where $\Omega_0 \equiv (eE_0/mc\omega)$ is the rest mass gyrofrequency, $\eta \equiv kc/\omega$ is the index of refraction, $\varepsilon \equiv eE_0/mc\omega$ is the dimensionless electric field strength, and the de-dimensionalized variables are $\theta \equiv \omega t$ and $X \equiv \omega x/c$. The parameter ε can be

estimated by Poynting flux arguments. In most devices, including EBT, ε is a very small parameter ($\sim 5.0 \times 10^{-5}$), thus permitting the use of perturbative techniques.

A multiple time scale analysis[8] is used with the slow time scale given by $\tau \equiv \varepsilon\theta$. With $\omega = (2\Omega_o/\gamma_i)$, the equations give to lowest order:

$$\Psi_o(\theta,\tau) \equiv \frac{\Omega_o}{\omega} \int^{\theta} \frac{d\theta}{\gamma_o(\varepsilon\theta)} + \Phi(\tau)$$

$$X_o(\theta,\tau) = \frac{2u_{\perp o}(\tau)}{\gamma_i} \sin \psi_o + X_G \ .$$

The guiding center position X_G in this equation can be shown to be constant in a Lagrangian formalism, to this order, and will be taken to be zero for simplicity. Also, γ_i is a constant tuning factor ($\simeq 1$). The subscript zero on the variables $u_\perp$, Ψ, and X refers to lowest order quantities in the time scale expansion.

The equations for $u_{\perp o}$ and Ψ_o are obtained by going to next order in the small ε expansion. To this order the sum of the integral of slowly varying terms must be zero to prevent secular growth in the perturbed quantities. Making use of the Bessel function expansion $\sin(x \sin(\theta) + y) = \sum_{-\infty}^{\infty} J_\ell(x) \times \sin(\ell\theta + y)$, using a small gyroradius expansion for the Bessel functions, and reinstating the dimensionality, the reduced constraint equations become, to lowest order in $k\rho$:

$$\frac{du_{\perp o}}{dt} = - \frac{\varepsilon k c}{2\gamma_i} u_{\perp o} \sin[\zeta(t) + 2\Phi(t)] \ , \tag{3}$$

$$\frac{d\zeta}{dt} = \frac{2\Omega_o}{\gamma_i} \left[\frac{\gamma_i}{\gamma_o(t)} - 1\right] \ , \tag{4}$$

$$\frac{d\Phi}{dt} = -\frac{\varepsilon k c}{2\gamma_i} \cos[(\zeta(t) + 2\Phi(t)] \ . \tag{5}$$

Equation (3) describes the perpendicular velocity evolution, Eq. (4) describes the phase change due to the relativistic mass shift, which becomes important for energy changes on the order of εmc^2, and Eq. (5) describes the evolution of the non-relativistic wave-particle phase. In the mildly relativistic limit, the above equations may be solved due to the fact that the second derivative of the phase, $\zeta + 2\Phi$, has only a weak velocity dependence and hence terms of order $u_{\perp o}^4/\varepsilon$ have been neglected. The excursion time, τ_{ex}, and energy, ξ_{ex}, as shown in Fig. 1c are found to be:

$$\tau_{ex} \simeq \frac{4}{\varepsilon\omega(AE)^{1/4}} K\left[\left(\frac{1}{2} - \left(\frac{D}{2(AE)^{1/2}}\right)\right)^{1/2}\right] \tag{6}$$

$$\xi_{ex} \simeq (\gamma_m - 1)mc^2 \frac{A^{1/2} - E^{1/2} + 2\eta}{E^{1/2} - \frac{\gamma_i - 1}{\varepsilon} - \eta} \ , \tag{7}$$

provided $(\gamma_i - 1) < (\gamma_m - 1)/2 + \eta\varepsilon$, and $(\gamma_m - 1) + (\xi_{ex}/mc^2) << (\varepsilon)^{1/2}$ where $A \equiv [\eta - ((\gamma_i - \gamma_m)/\varepsilon)]^2$, $E \equiv A + (4(\gamma_i - 1)\eta/\varepsilon)$, $D \equiv ((\gamma_i - \gamma_m)/\varepsilon)^2 + (2(\gamma_m - 1)\eta/\varepsilon) - \eta^2$, γ_m is the minimum value of γ_o during an energy excursion, and the function K is the complete elliptic integral of the first kind. These conditions were chosen so that the phase remains a monotonic function during the energy excursion. It should be noted that while γ_m is always greater than 1, γ_i is a tuning factor which may be less than 1. These formulae compare with the full numerical solution to within 40% so long as the above weak relativity and phase monotonicity inequalities are satisfied and wave polarization is accounted for.

To phenomenologically estimate the heating coefficient in Fig. 3 utilizing these analytic results, an estimate of the effective randomization frequency is required. The phase slippage correction due to unperturbed parallel motion in a parabolic magnetic well is on the order of $(v_\parallel/v)^2$ at the midplane. By adding such a correction to Eq. (4), it is observed that when $(v_\parallel/v)^2$ is greater than the change in γ due to the excursion, ξ_{ex}/mc^2, the parallel motion begins to dominate the nonlinear relativistic effects. Collisional changes in $(v_\parallel/v)^2$ on the order of ξ_{ex}/mc^2 are thus characteristic of the randomization required to significantly change the energy excursion behavior. The effective randomizing frequency can thus be estimated using $\nu_{eff} = \nu_\perp/(\Delta\kappa)^2$ with $(\Delta\kappa)^2 \simeq \xi_{ex}/mc^2$.

An estimate of the heating coefficient can now be made with a diffusive model in velocity space in analogy with banana orbit diffusion in tokamaks. Consider a diffusion equation of the form

$$\frac{\partial f}{\partial t} = \frac{1}{2} \frac{\langle(\Delta v)^2\rangle}{\Delta t} \frac{\partial^2 f}{\partial v^2}$$

where f is the distribution function and Δv is the typical diffusive change in velocity on a Δt time scale. For kinetic energy $T = mv^2/2$, ΔT is $mv\Delta v$ and the average change in energy is described by:

$$\frac{\partial\langle T\rangle}{\partial t} \simeq \frac{1}{4\langle T\rangle} \frac{\langle(\Delta T)^2\rangle}{\Delta t} .$$

By equating this $\partial\langle T\rangle/\partial t$ to the absorbed power in Eq. (2) and using $k\rho = 2v/c$ near the second harmonic frequency, the estimate for α is given by:

$$\alpha \simeq \frac{\pi m^2 c^2 \omega}{4e^2 |E_+|^2} \frac{1}{\langle T \rangle^2} \frac{\langle (\Delta T)^2 \rangle}{\Delta t} \cdot \tag{8}$$

For the "collisional" regime where $\nu_{eff} >> \nu_{ex}$, energy changes of roughly $\xi_{ex}\nu_{ex}/\nu_{eff}$ occur with frequency $\nu_{eff} = 1/\Delta t$. Substituting these into Eq. (8), the "collisional" heating efficiency is given by:

$$\alpha \simeq \frac{\pi m^2 c^2 \omega \nu_{ex}}{4e^2 |E_+|^2} \left(\frac{\xi_{ex}}{\langle T \rangle}\right)^2 \left(\frac{\nu_{ex}}{\nu_{eff}}\right) \qquad \nu_{eff} >> \nu_{ex} \cdot \tag{9}$$

In the "collisionless" regime, energy changes on the order of ξ_{ex} occur with frequency ν_{eff}. From Eq. (8), the "collisionless" heating efficiency is given by:

$$\alpha = \frac{\pi m^2 c^2 \omega \nu_{ex}}{4e^2 |E_+|^2} \left(\frac{\xi_{ex}}{\langle T \rangle}\right)^2 \left(\frac{\nu_{eff}}{\nu_{ex}}\right) \qquad \nu_{ex} >> \nu_{eff} \cdot \tag{10}$$

These formulas along with Eqs. (6) and (7) describe the dashed curves shown in Fig. 3.

The results of this analysis may also be applied to ions if the wave properties at twice the ion cyclotron frequency are considered. The product εkc at these frequencies is usually much smaller, resulting in much longer energy excursion times; hence, Coulomb collisional effects, particle drifts or other mechanisms may complicate the second harmonic cyclotron interaction. The product εmc^2 for ions, however, may be on the order of a few keV, so that relativistic detuning is a slower process. Thus, the relativistic energy excursion effect for ions is expected to occur on a much longer time scale with the maximum energy attained during an excursion on the order of keV greater than

the minimum energy, provided no other processes occur on the excursion time scale and the small gyroradius expansion does not break down.

A finite bandwidth ($\Delta\omega/\omega$), may also be important for ions if $\Delta\omega/\omega$ is of the same order as ε. (For the second harmonic electron cyclotron frequencies produced by gyrotrons in EBT, $\Delta\omega/\omega$ is typically much less than ε.)

In summary, nonlinear relativistic effects are very important for electrons trapped near a second harmonic cyclotron resonance, even at very low energies. The resulting energy excursion behavior can provide significant heating and high energy tail formation in low energy electron distribution functions, provided a phase randomizing mechanism exists. The excursion time, the change in energy during an excursion, and the consequent heating have been calculated analytically in a mildly relativistic approximation.

Acknowledgments

The authors would like to thank Dr. W.M. Nevins at LLNL for helpful discussions and to note that Dr. Nevins has independently derived formulae for the energy excursion processes. The authors would also like to thank Dr. J.S. Tolliver and Dr. J.A. Rome for helpful discussions on the use of vectorizable computers and Dr. L.W. Owen for advice on particle following routines. One of the authors (MDC) gratefully acknowledges the support by the Fusion Energy Division at Oak Ridge National Laboratory for a summer visit during which this project was initiated. This work was supported by the U.S. Department of Energy, Office of Fusion Energy under Contract DE-AC02-80ER53104 (University of Wisconsin) and w-7405-eng-26 with Union Carbide Corporation (Oak Ridge National Laboratory).

References

1. D.B. Batchelor, Proceedings of the Workshop on EBT Ring Physics, Dec. 3-5, 1979, Oak Ridge TN, p. 261, published by Oak Ridge National Laboratory, Oak Ridge, TN, Conf-791228 April, 1980.
2. N.A. Uckan and EBT Group, Plasma Physics 25, 129 (1983).
3. J.Y. Hsu and S.C. Chiu, Phys. Rev. Letters 45, 1561 (1980)
4. B.A. Trubnikov, "Particle Interactions in a Fully Ionized Plasma", Reviews of Plasma Physics, Vol. 1 (Consultants Bureau, New York, 1965), p. 105.
5. R. Shanny, J.M. Dawson and J.M. Greene, Phys. Fluids 10, 1281 (1967).
6. G.E.P. Box and M.E. Muller, Ann. Math. Statist. 29, 610 (1958).
7. T.D. Rognlien, Phys. Fluids 26, 1545 (1983).
8. C.M. Bender and S.A. Orszag, Advanced Mathematical Methods for Scientists and Engineers (McGraw-Hill, New York, 1978).

Figure Captions

Fig. 1. The evolution of electron energy for different midplane values of $v_{\parallel}/v$ with no collisions. In all cases $|E_+|$ = 193 V/cm at 18 GHz with the second harmonic resonance at the midplane.

(a) The energy evolution of an electron with $v_{\parallel}/v \simeq 0.4$ in a typical stochastic interaction with the second harmonic resonance.

(b) An example of an electron making a transition between "stochastic" and "excursion" behavior, with the initial $v_{\parallel}/v \simeq 0.1$.

(c) Typical energy excursion behavior observed when an electron is trapped in the second harmonic resonance with $v_{\parallel}/v = 0.0$.

Fig. 2. A snapshot of velocity space after 0.3 microseconds illustrating the regions where energy excursion interactions are important. Initially, all electrons were at 26 eV with randomized phases and $v_{\parallel}/v$ randomized between 0.0 and 0.6. $|E_+|$ = 193 V/cm at 18 GHz with the second harmonic resonance at the midplane.

Fig. 3. The coefficient of second harmonic power absorption for a wide range of collisionality, with $\nu_{ex} \equiv 1/\tau_{ex}$, $(\Delta\kappa)^2 = 5 \times 10^{-4}$. All quantities were calculated based upon the average energy of only those electrons with $v_{\parallel}/v$ less than 0.2. The dashed curves show the analytic estimates given by Eqs. (9) and (10).

Fig. 4. The energy distribution of 64 electrons averaged over the last microsecond of simulation, after 9 microseconds of evolution. The 150 eV Maxwellian background scattering distribution is shown as a dashed curve. Initially all electrons were at 205 eV with phases and pitch angles randomized. $|E_+| \equiv 64$ V/cm at 18 GHz, background density = 3×10^{11} cm^{-3}, and a mirror ratio of 2.8.

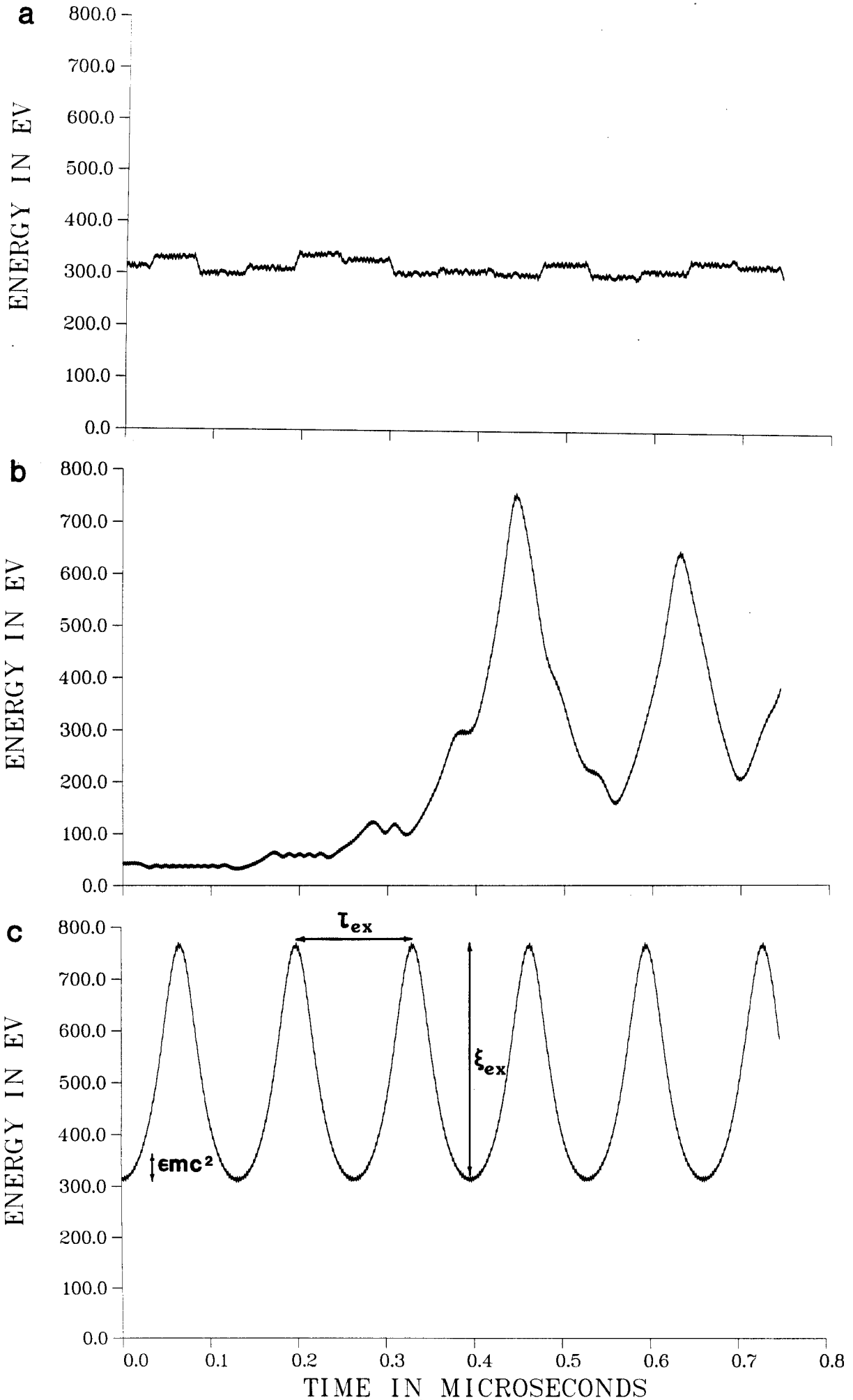
a
b
c
ENERGY IN EV
800.0
700.0
600.0
500.0
400.0
300.0
200.0
100.0
0.0
τ_{ex}
ξ_{ex}
ϵmc^2
0.0
0.1
0.2
0.3
0.4
0.5
0.6
0.7
0.8
TIME IN MICROSECONDS

Figure 1

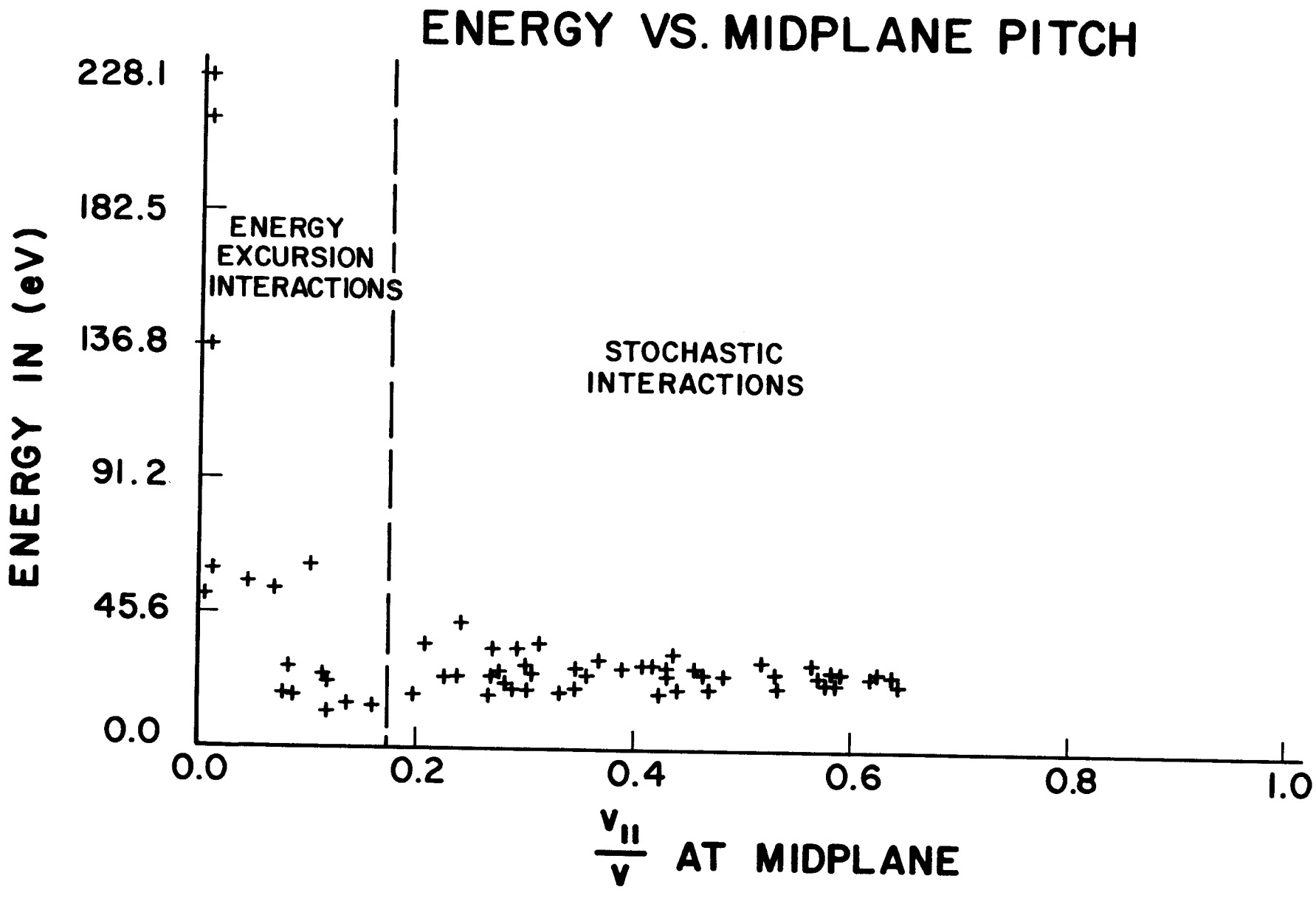
ENERGY VS. MIDPLANE PITCH
228.1
182.5
136.8
91.2
45.6
0.0
ENERGY IN (eV)
ENERGY EXCURSION INTERACTIONS
STOCHASTIC INTERACTIONS
0.0
0.2
0.4
0.6
0.8
1.0
$\frac{v_{\parallel}}{v}$ AT MIDPLANE

Figure 2

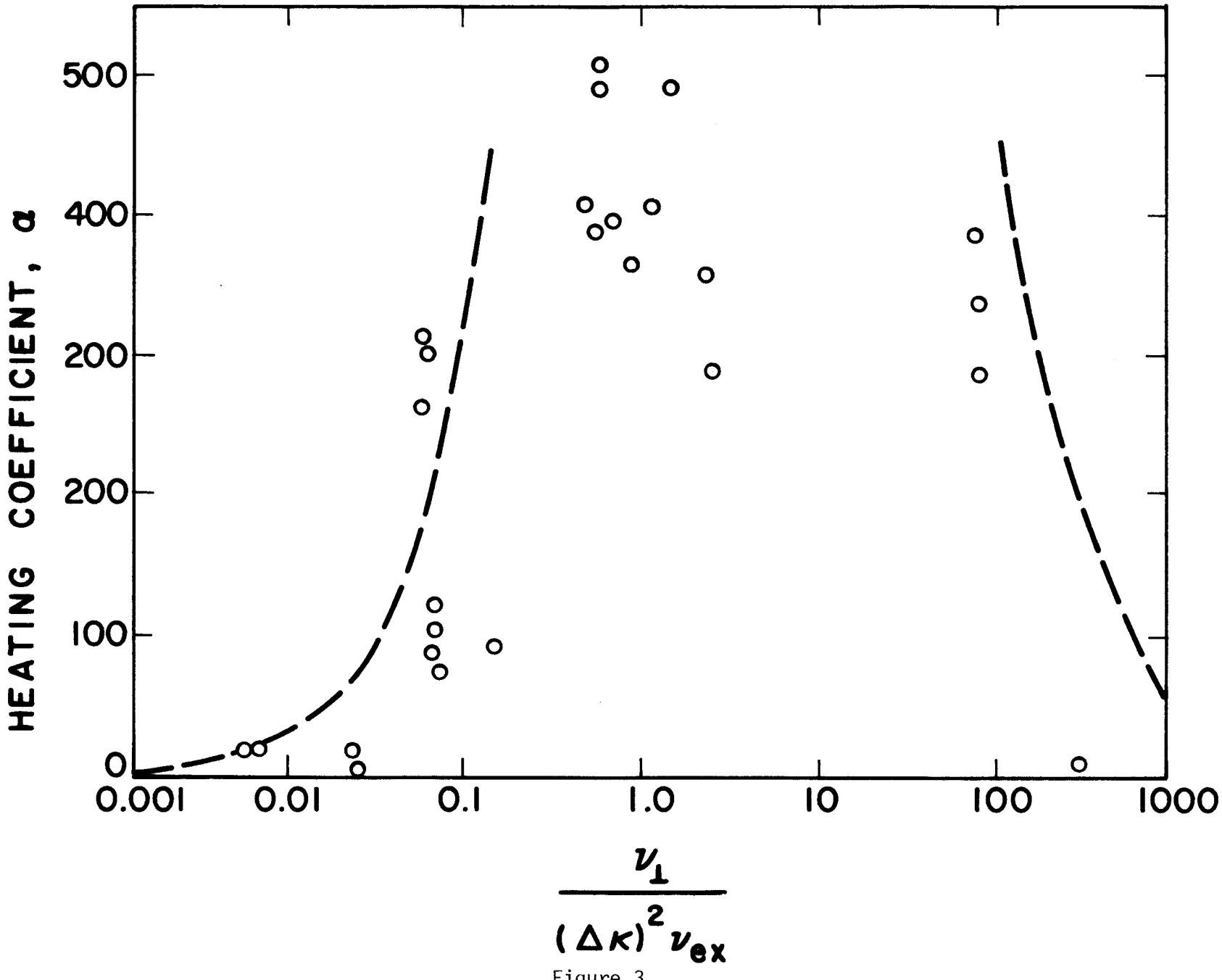
HEATING COEFFICIENT, α
500
400
200
200
100
0
0.001
0.01
0.1
1.0
10
100
1000
$\frac{\nu_\perp}{(\Delta\kappa)^2 \nu_{ex}}$

Figure 3

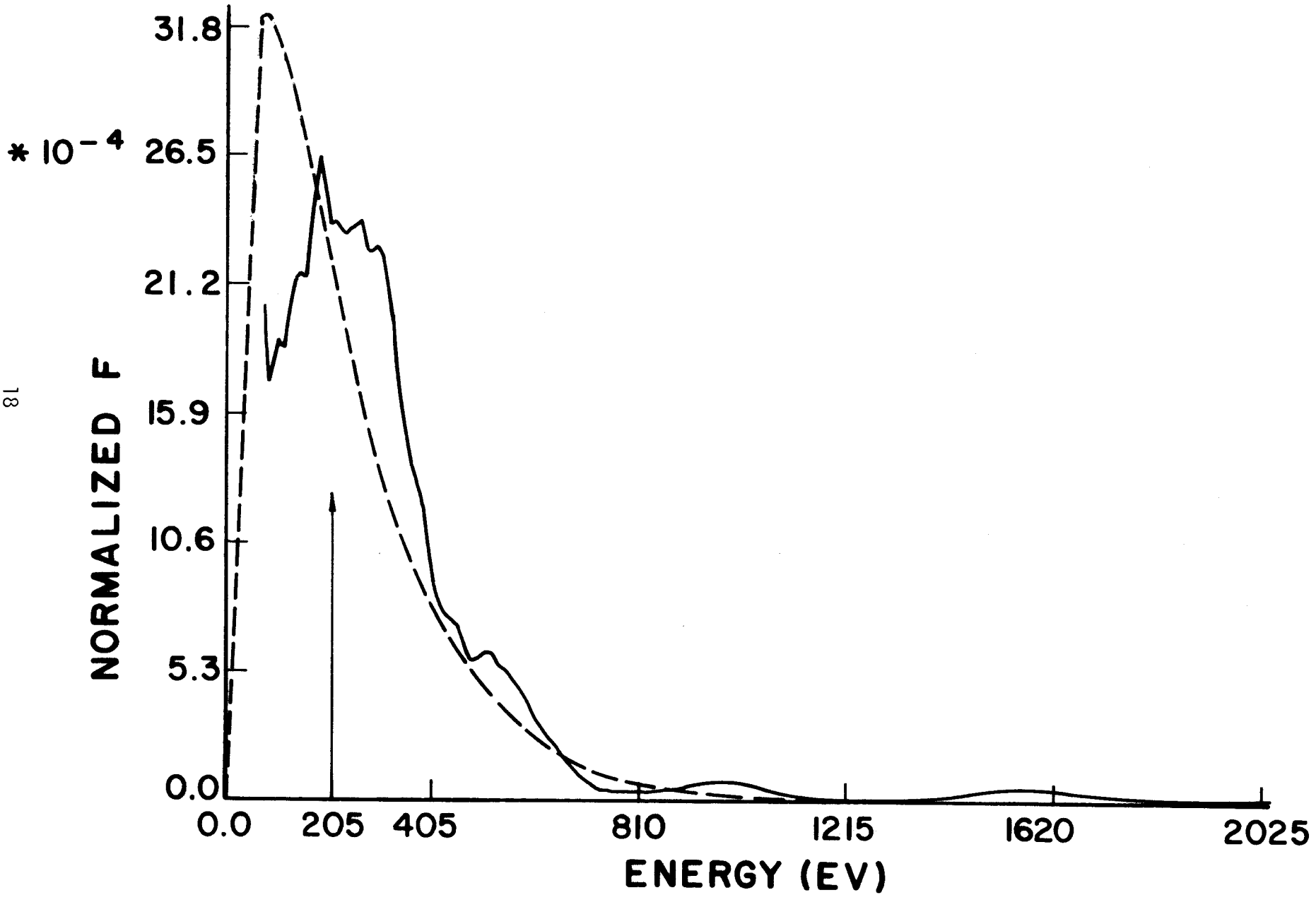
31.8
26.5
21.2
15.9
10.6
5.3
0.0
* 10⁻⁴
NORMALIZED F
0.0
205
405
810
1215
1620
2025
ENERGY (EV)

Figure 4